THE ASTROPHYSICAL JOURNAL, 515:746–761, 1999 April 20
© 1999. The American Astronomical Society. All rights reserved. Printed in U.S.A.

EXTREME ULTRAVIOLET EXPLORER PHOTOMETRY OF RS CANUM VENATICORUM SYSTEMS: FOUR FLARING MEGASECONDS

RACHEL A. OSTEN AND ALEXANDER BROWN
Center for Astrophysics and Space Astronomy, University of Colorado, Boulder, CO 80309-0389;
raosten@casa.colorado.edu, ab@echidna.colorado.edu
Received 1998 March 23; accepted 1998 December 1

ABSTRACT

We present an analysis of 12.2 Ms of *Extreme Ultraviolet Explorer* (*EUVE*) photometry of 16 RS CVn systems (including four flaring megaseconds). Our study attempts a systematic categorization of stellar coronal emission in RS CVn binary systems. The temporal resolution of the *EUVE* satellite and the opportunity for long observations enables us to study separately the quiescent and flaring states of RS CVn systems. Thirty of 31 observations are statistically variable. We examine light curves, characterizing both phase-dependent variations and large- and small-scale flaring. There is evidence for small-scale stochastic variability on the one short-period ($P_{\rm orb} < 1$ day) system in our sample (ER Vul), which we interpret as small-scale flaring. CF Tuc is the only system for which phase-dependent variations over multiple orbital periods are seen. We analyze 30 flares on nine systems, fitting rise and decay times. Several flares have durations $>0.5P_{\rm orb}$ and thus cannot originate from compact emission regions close to the stellar surfaces. Many flares have unusual flare morphologies, with rise times comparable to or greater than the decay time, and emission plateaus. In addition, eight flares have decay phases that are fit better by a broken power law than a single power law. The decay times for the second power law are statistically different than the single decay times and are correlated with the flare rise times. This observed connection points to the potential importance of the change in decay rate as a means of examining the physical processes operating during the flare. The distribution of orbital phases of flare onsets on V711 Tau (HR 1099), the best-studied RS CVn in our sample, is consistent with a Poisson distribution that is random in time. In two systems that are partially eclipsing (CF Tuc and ER Vul), we find no evidence for an eclipse in the light curve, indicating that the emission region is large compared to the stellar radius. We parameterize the distribution of flare energies as a power law, finding a cut-off energy of $\approx 10^{33}$ ergs and a slope of -0.6. Flare energy increases with flare duration as $E \propto \Delta t^{1.42}$, confirming the long-duration nature of high-energy flares on RS CVn systems. The integrated flare luminosity depends on the quiescent luminosity as $L_{\rm flare} \propto L_{\rm quiescent}^{1.05}$. Flare frequencies range from 0.1 day^{-1} to 1.5 day^{-1}. For observations not affected by the dead spot on the Deep Survey detector, 40% of the observed time was spent in a flaring state, indicating that flaring is a "normal" state for the coronae of these systems. We note the presence of a quasi-periodicity in *EUVE* photometric data on the order of 1 day, which is not corrected for in the standard reduction and analysis software.

Subject headings: binaries: close — stars: activity — stars: coronae — stars: late-type — ultraviolet: stars — X-rays: stars

1. INTRODUCTION

RS CVn systems are detached binary systems, usually composed of an evolved star and a main-sequence star, in which tidal effects enhance chromospheric and coronal activity (Hall 1976). They are the most active late-type binary systems; the levels of chromospheric and coronal emission are saturated (Vilhu & Walter 1987). Their rapid synchronous rotation ($P_{\rm rot} < 25$ days) powers intense high-energy emission. Indeed, flux levels in the extreme ultraviolet (EUV) and X-ray are several orders of magnitude greater than those of slowly rotating, single late-type stars, and RS CVn systems are the brightest coronal X-ray sources. Newly discovered RS CVn systems are often identified first in the EUV and X-ray, e.g., the recent all-sky surveys of *EUVE* and *ROSAT* (Mitrou et al. 1997; Dempsey et al. 1993a). Optical studies of RS CVn systems show the presence of large, cool photospheric spots, reminiscent of sunspots but covering a much larger fraction of the stellar disk (Hatzes et al. 1996; Vogt et al. 1999). Photospheric magnetic fields measured on these systems are in the range 1–2 kG, with filling factors over 50% (Giampapa, Golub, & Worden 1983; Bopp et al. 1989). It is believed that the fast rotation drives a dynamo that produces the observed atmospheric phenomena.

White, Sanford, & Weiler (1978) reported the first X-ray flare on an RS CVn binary (V711 Tau). Since then, RS CVn's have been shown to flare frequently in the X-ray, EUV, ultraviolet (UV), optical, and radio (Byrne 1989; Linsky 1991). The energy released in flares on RS CVn's can be 4–5 orders of magnitude greater than in solar flares, e.g., 10^{37} ergs (Kürster & Schmitt 1996) compared to a typical 10^{32} ergs on the Sun. Multispectral region studies of RS CVn systems show that soft X-ray and EUV emission is sensitive to the gradual flare phase, while nonthermal radio gyrosynchrotron emission responds to the impulsive phase (Brown et al. 1996; Jones et al. 1996). While the exact flaring process is not known, it is thought to involve regions of magnetic shear (Zirin, MacKinnon, & McKenna-Lawlor 1991) that produce magnetic reconnection and energy release. There is evidence (Zhai et al. 1994; Catalano & Frasco 1994) that suggests a correlation between spot development and flare occurrence. The notion that stellar flare phenomena may be different from solar flares arises from the large difference in energy release, coupled with vastly

different rotational periods, starspot coverages, and possibly even magnetic fields.

Observations of RS CVn systems at soft X-ray wavelengths reveal a complex coronal structure: electron densities in the range 10^{12}–10^{13} cm^{-3} (Schrijver et al. 1995) and subsolar abundances (Ortolani et al. 1997; Singh, White, & Drake 1996; Schmitt et al. 1996) that change with activity level (Güdel et al. 1999). Typical plasma temperatures lie in the range 2–20 $\times$ 10^6 K (Schrijver et al. 1995); during a flaring state temperatures can be as high as 10^8 K (Ottmann & Schmitt 1994; Güdel et al. 1999). Long duration flares (>1.5 days) have been detected (Endl, Strassmeier, & Kürster 1997; Kürster & Schmitt 1996; Ottmann & Schmitt 1994). Phase-dependent emission variations have been tentatively identified (Drake et al. 1994; Gunn et al. 1997). The large volume emitting regions implied in some flare analyses (Mewe et al. 1997; Kürster & Schmitt 1996) have led to speculation of intrabinary activity (Gunn et al. 1997).

Solar flares are typically classed as either compact flares, with short time durations and small energy releases, or as two-ribbon flares, which demonstrate longer durations and larger energy releases. Compact flares tend to occur only on a single coronal loop, whereas two-ribbon flares happen in an arcade of loops (Pallavicini, Serio, & Vaiana 1977). On the Sun, two-ribbon flares are preceded by the eruption of a filament (Haisch, Strong, & Rodonò 1991). This leads to particle acceleration in the coronal loop downward into the chromosphere, where the chromospheric material heats and is evaporated, filling up the coronal loop. The impulsive phase of the flare corresponds to particle injection into the chromosphere, while the "gradual" phase describes the filling of the coronal loop and subsequent radiation. Flare scenarios still lack an explanation of what triggers the flare, what the cooling mechanism is, and the overall energy budget for a flare. Studies of flares on solar neighborhood stars reveal phenomena similar to both compact and two-ribbon flares (Pallavicini, Tagliaferri, & Stella 1990). Time-dependent magnetic reconnection models developed for solar two-ribbon flares have been applied to flares on RS CVn systems (e.g., II Peg; Mewe et al. 1997).

The advantage of the *Extreme Ultraviolet Explorer* (*EUVE*) satellite in studying coronal sources is its ability to observe for long time intervals. Previous systematic studies of RS CVn systems have had large sample sizes but relatively poor temporal resolution. Observations that extend over multiple orbital periods can address questions such as rotational modulation, flare frequencies, and preferential flaring phases. This paper studies flare phenomena on RS CVn systems in the EUV spectral region (70–250 Å). By looking at many systems with long observations, we hope to shed light on the following questions.

1. How frequently do RS CVn systems flare? What is the range of flaring behavior?
2. Is there evidence of phase-dependent variations in these long observations?
3. What are the characteristics of EUV flares on RS CVn systems? How do they compare to solar coronal flares, and flares from single flare stars?
4. Is there any relation between flare properties and physical properties of the system?

We present an analysis of EUV photometry of 16 RS CVn systems made with the *EUVE* encompassing 12.2 Ms of *EUVE* satellite time. Spectroscopy obtained during most observations will be presented in later papers. Section 2 describes the data reduction. Phase-dependent variability and small-scale variability of the light curves are addressed in § 3, while the large-scale flares are discussed in § 4. Section 5 is a summary of our investigations.

2. DATA REDUCTION AND ANALYSIS

2.1. *DS/S and RAP Reduction*

The *EUVE* satellite (Malina & Bowyer 1991) acquires data with the Deep Survey Detector and Spectrometer assembly (DS/S) and three all-sky monitors that provide scanner photometry. The telescopes have a roughly 2° field of view and ≈30% observing efficiency. The Lexan/boron filter on the Deep Survey imager (Malina et al. 1994; Bowyer et al. 1994) has a bandpass of 80–180 Å, with a peak effective area of ∼29 cm^2 at 90 Å. The Right Angle Program (RAP) utilizes the three all-sky monitors. The scanner telescopes have a field of view of 5° diameter and four quadrants per mirror, two of which have Lexan/boron filters (60–180 Å, peak effective area ≈12 cm^2 at 93 Å), and the other two having aluminum/carbon filters (170–240 Å, peak $A_{\rm eff}$ ∼ 4 cm^2 at 170 Å). Data were obtained from DS/S and RAP observations, both archival and proprietary.

The data were processed with the standard *EUVE* General Observer (EGO) software within the Image Reduction and Analysis Facility (IRAF).[1] Reference data sets used for data reduction were those available at the time of each observation. Corrections were made for detector dead time and "primbsching" described in Miller-Bagwell & Abbott (1995),[2] and for vignetting in RAP observations. Source and background extraction and light curve calculation were performed using our own IDL software procedures (see, e.g., Gagné et al. 1999). The source count rates were higher than background count rates, allowing easy visual identification of the source. A source region was determined by a circle around the source, large enough to enclose all source photons; the background region was defined by an annulus around the source circle. Data were binned into 3000 s intervals (approximately one point per satellite orbit) for initial analysis; subsequent flare analysis was conducted on light curves binned into 500 s intervals (six points per satellite orbit). Details of the observations are given in Table 1. We find it useful to define a quantity $N_{\rm orb}$, which gives the total number of stellar orbital periods encompassed by our *EUVE* observations. We compute $N_{\rm orb}$ according to

$$N_{\rm orb} = \left(\frac{T_{\rm elapsed}}{P_{\rm orb}}\right) = \frac{(T_{\rm exp}/\epsilon)}{P_{\rm orb}},$$

where ϵ is the observing efficiency of the satellite (30%; Miller-Bagwell & Abbott 1995). Spectral types and orbital period are taken from Strassmeier et al. (1993, hereafter CABS). Light curves are shown in Figures 1, 2, 3, and 4.

[1] IRAF is distributed by the National Optical Astronomy Observatories, which is operated by the Association of Universities for Research in Astronomy, Inc., under contract to the National Science Foundation (USA).

[2] The *EUVE* Guest Observer Center Data Products Guide is available on-line at http://w3.cea.berkeley.edu/science/html/Resources_pubs_datapg.html.

TABLE 1

SUMMARY OF *EUVE* OBSERVATIONS WITH SYSTEM PROPERTIES

System	Spectral Type[a]	P_{orb}[a] (days)	N_{orb}	Observation Date (YY/MM)	T_{exp} (ks)	DS/S or RAP	Flares?	$P_{constant}$[b]
ER Vul	G0 V/G5 V	0.698	5.1	1993/09	184	DS/S	n	0
			9.8	1995/07	177	RAP	n	0.367
σ^2 CrB	F6 V/G0 V	1.14	2.8	1994/02	84	DS/S	y	0
V824 Ara	G5 IV/K0 V–IV	1.68	0.8	1996/05	36	DS/S	y	0
V815 Her	G5 V/M1–2 V	1.81	1.4	1996/06/15	66	RAP	y	0
			0.8	1996/06/25	40	RAP	y	0
EI Eri	G5 IV/??	1.95	0.3	1995/11	15	RAP	n	0.130
AR Lac	G2 IV/K0 IV	1.98	1.6	1993/10[c]	80	DS/S	y	0
BH CVn	F2 IV/K2 IV	2.6	2.5	1996/02[c]	170	DS/S	y	0
CF Tuc	G0 V/K4 IV	2.8	3.79	1994/08	142	DS/S	n	0
V711 Tau	G5 IV/K1 IV	2.84	0.6	1992/10	47	DS/S	n	5×10^{-7}
			1.0	1993/09	80	DS/S	y	0
			0.8	1994/08	56	DS/S	y	0
			2.7	1996/09	198	DS/S	y	0
			3.8	1996/10	278	RAP	y	0
ξ UMa	G5 V/??	3.98	0.4	1993/03	37	DS/S	n	0
			1.9	1996/02	193	RAP	n	0.996
UX Ari	G5 V/K0 IV	6.44	0.5	1994/10[c]	79	DS/S	y	0
			0.5	1995/11/7	85	DS/S	y	0
			0.6	1995/11/19	107	DS/S	y	0
II Peg	K2–3 V–IV/??	6.72	0.5	1993/10[c]	94	DS/S	y	0
			0.6	1995/08	96	DS/S	y	0
			1.2	1995/10	202	RAP	y	0
			0.9	1996/11	165	RAP	n	5×10^{-6}
VY Ari	K3–4 V–IV/??	13.2	0.4	1994/10[c]	154	DS/S	n	0
			0.1	1996/09	21	RAP	n	0
			0.2	1996/10	67	RAP	y	0
AR Psc	K2 V/??	14.3	1.1	1997/08	349	DS/S	y	0
σ Gem	K1 III/??	19.6	0.1	1993/02[c]	44	DS/S	n	0
λ And	G8 IV–III/??	20.52	0.1	1993/10[c]	56	DS/S	y	0
			1.2	1997/07	263	DS/S	y	0

[a] Spectral type and orbital period are taken from CABS.
[b] Probability that the light curve fits its mean value, taken from the χ^2_ν probability distribution.
[c] Observation was contaminated by dead spot on DS/S detector.

2.2. *The EUVE Dead Spot*

Several observations were contaminated wholly or partly by the dead spot on the DS detector (Miller-Bagwell & Abbott 1995). The dead spot is a symmetric area on the detector of decreased sensitivity (20%–85%) and roughly 2′ in size, created during a long exposure of the bright EUV source HZ 43 in 1993 January. After 1993 October, all observations were pointed 1.′5–2′ off axis to avoid exposure in the dead spot. However, several of our observations from 1993 showed partial or total contamination by the dead spot. Spacecraft pointing relative to the dead spot was determined for all light curves; intervals of observing time affected by the dead spot were discarded. Observations affected by the dead spot are noted in Table 1; these systems are: AR Lac, UX Ari (1993 October), II Peg (1993 October), VY Ari (1994 October), σ Gem, λ And (1993 October), and BH CVn. These light curves are marked with asterisks in Figures 1, 2, 3, and 4.

2.3. *Quasi-Periodicity in Light Curve Data*

In our analysis of other *EUVE* data, we have detected a quasi-periodic light curve modulation of $\sim$1 day, unaccounted and uncorrected for by present EGO data reduction techniques. This quasi-periodic signal persists even after the most careful data filtering and background subtraction. There is no description of this effect in any EGO manuals. We note two other papers that have detected periodicities in *EUVE* data on the order of 1 day: in the Seyfert galaxy RX J0437.4−4711 (Halpern & Marshall 1996) and in the single dwarf F8 star HD 35850 (Gagné et al. 1999). Halpern & Marshall (1996) find a period of 0.901 days in their data, while Gagné et al. (1999) find a period of 0.98 days in their observations. Halpern & Marshall note no power in their periodogram at timescales around 0.98 days, the period of passages through the South Atlantic Anomaly (SAA), but they do note a strong modulation of the dead-time correction factor at this period. The 0.91 day period is probably far enough from 1 day not to be considered spurious (J. P. Halpern 1998, private communication). We find a similar period of $\sim$1 day in light curves of Capella, a G1 III/G8 III binary system. We advise caution when examining DS/S light curves for periods on the order of 1 day—there may be satellite effects that have not been accounted for in the reduction. The implication of the quasi-periodicity has ramifications on any attempt to interpret light curve modulation as due to the source.

Our flare analysis seeks an exponential rise and decay in the light curve (see below). We feel that this adequately separates possible satellite-induced modulation from intrinsic flare modulation of the light curve. The systems whose

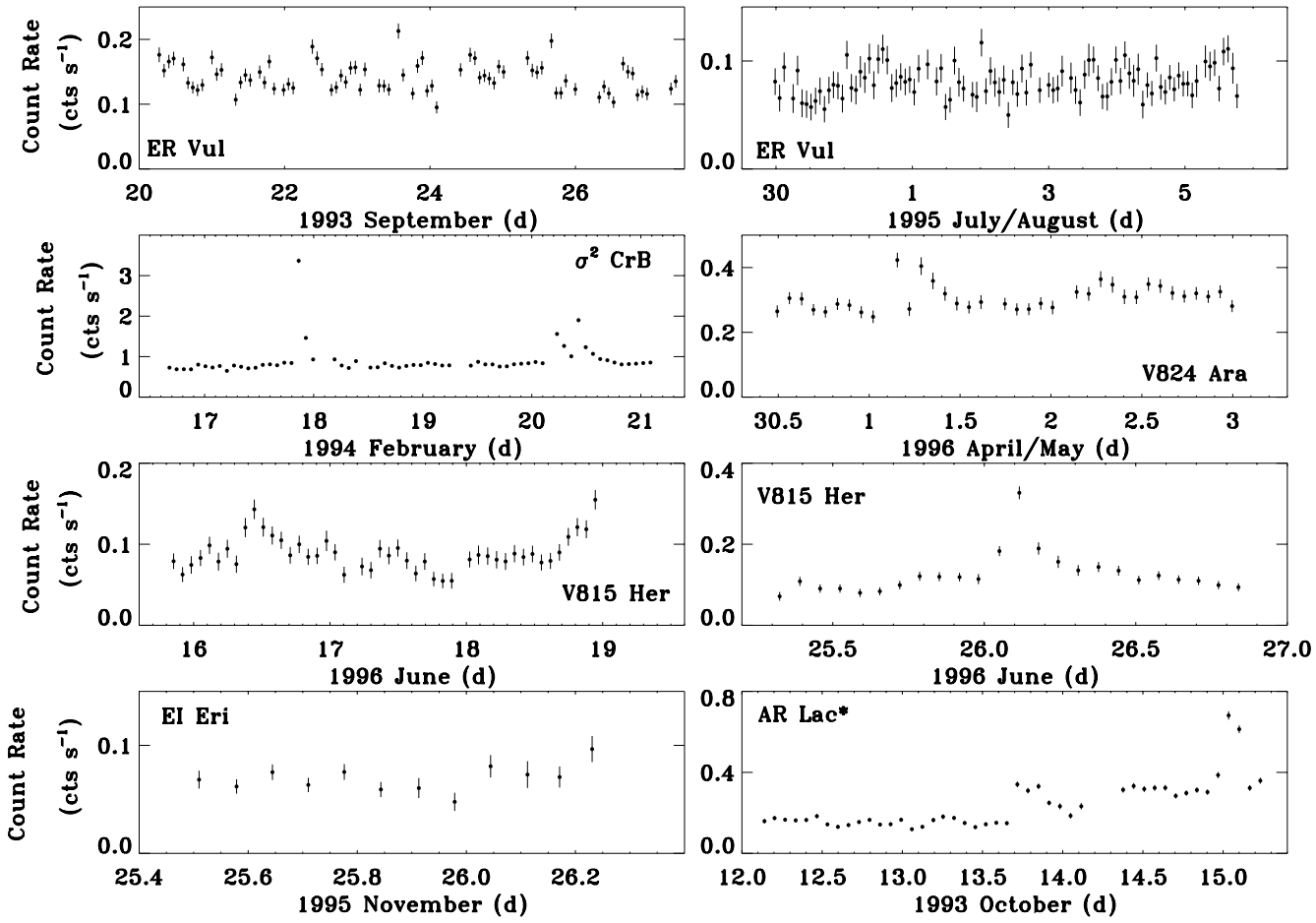


FIG. 1.—EUV light curves for RS CVn binaries, ordered by increasing orbital period. Each point represents one satellite orbit. Error bars are 1 σ. Light curves with an asterisk next to the identifier were contaminated by the dead spot on the Deep Survey detector; see text for details.

observations permit examination of phased modulation are either shorter ($P_{\rm orb} \approx 0.7$ days) or much longer than 1 day, so we are confident that any subsequent attempts to explain modulation in these systems is due to the source itself and not a satellite-induced modulation.

3. LIGHT CURVE VARIABILITY

To assess light curve variability, we used a statistical test of variation from the mean count rate. The χ^2_ν probability was then used to determine whether the light curve demonstrated significant variability. For 30 of the 31 observations, there was statistical evidence of variability (see Table 1). In characterizing nonflaring types of variability, we use the term "phase-dependent variation" as a general description of observed light curve variation that occurs at the same phase over multiple orbital periods. This phrase is general enough to encompass many types of variability, without being specific about the physical origin of the variation. We discuss a search for this variability in § 3.2. In contrast, eclipsing behavior has characteristic signatures that should be recognizable: the duration of eclipse as gleaned from optical light curves and specific phases at which eclipse variation should be seen. We report the results of a search for eclipsing behavior in the light curves in § 3.3.

3.1. *Evidence of Small-Scale Flaring on ER Vul*

We present evidence of small-scale flaring on the one short-period ($P_{\rm orb} < 1$ day) RS CVn system in our sample. The two light curves of ER Vul (1993 September and 1995 July) are variable, even though they do not contain large-scale flares. We investigated the hypothesis that many small-scale flares could be occurring stochastically, giving rise to the observed light curve. We examined the deviation from the mean count rate for each light curve and compared the distribution of such deviations with what would be expected from a Poisson distribution. Figure 5 overlays a Poisson distribution (*cross hatched region*) on the distribution of events on ER Vul (*thick line*). Each distribution is normalized to the total number of events. For events $<2\ \sigma$, the data seem to reproduce adequately the Poisson distribution. At $>2\ \sigma$, the distribution of variability in ER Vul departs from a nearly Poisson-like distribution. There are large gaps at 3.5–4 σ and 5–6 σ, where there are no data points, as well as much larger values of the distribution of data compared to the Poissonian distribution at 2.5–3 σ, 4–5 σ, and $>6\ \sigma$. The variability at $>2\ \sigma$ cannot be due to purely Poisson processes. We interpret this non-Poisson variability on ER Vul as due to small-scale, stochastic flaring.

The observations of ER Vul offer the most comprehensive orbital coverage, because of its small orbital period. We investigated the possibility that similar small-scale flaring could be occurring on other systems without being identified as such. An analysis of "quiescent" light curves of systems with smaller orbital-period coverage also reveals a non–Poisson-like distribution of variability. The

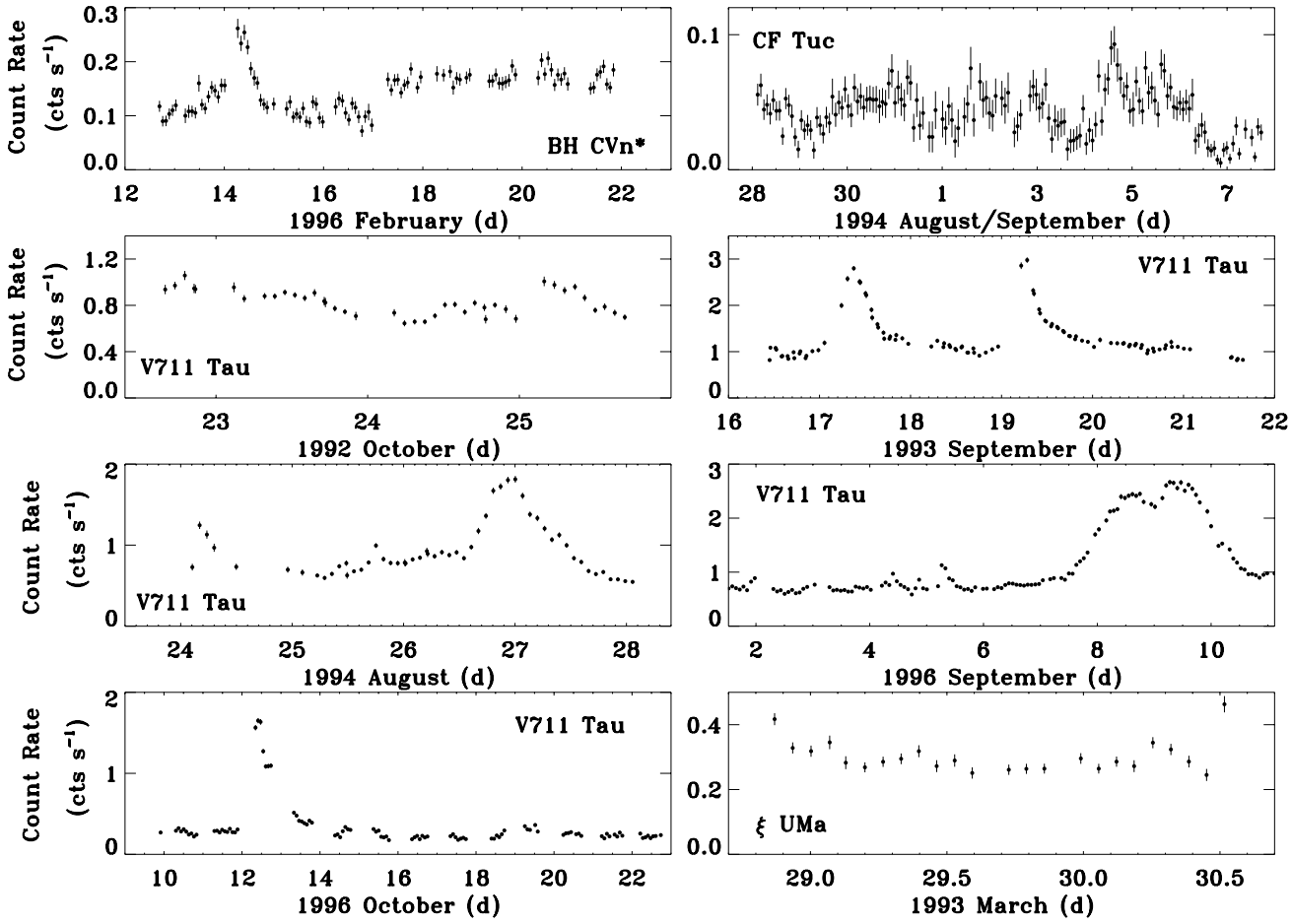


FIG. 2.—Same as for Fig. 1

peak luminosity observed in the ER Vul system is 4.7×10^{28} ergs s^{-1}. Table 2 lists the peak flare luminosity of the large-scale flares observed and analyzed individually on other systems. (The analysis of individual, large-scale flares is given in § 4.1.) A comparison between the ER Vul luminosity and the range of peak flare luminosities reveals that the peak ER Vul luminosity is on the low end of the range of individual large flare peak luminosities; only four individually observed flares have peak luminosities smaller than ER Vul's peak luminosity. We translated the observed peak luminosity on ER Vul into an expected count rate on V711 Tau, which shows quiescent emission as well as large-scale flares. The observed level of the small-scale flaring on ER Vul would not be distinguishable from the quiescent emission level on V711 Tau. The phenomenon we observe on ER Vul could, therefore, easily be present but remain unrecognized in systems in which large-scale flares do occur. This does not explain the lack of observed large-scale flares on ER Vul, however. Using the minimum observed flare frequency (discussed in § 4.3) of individual, large-scale flares of 0.1 day^{-1}, we would expect to see at least one large-scale flare during the 14.9 total orbital periods ($\approx$10 days) that the system was observed. The small timescale variability and small luminosities suggest that the flaring observed on ER Vul is indeed small-scale flaring, particularly when compared to the luminosities characteristic of large-scale flares. In addition, White et al. (1987) demonstrated variations of less than 50% amplitude on timescales of a few hours in their *EXOSAT* observations of ER Vul. These light curves are similar to the *EUVE* light curves presented here. The continuity in behavior of ER Vul in observations $\sim$10 yr apart suggests that the behavior is typical of this system. However, we cannot interpret the lack of similar observations on longer period systems as an absence of small-scale flaring on these systems, since the typical luminosities involved would not be distinguishable from what we interpret as "quiescence" in these systems.

The extremely fast rotation of the two stars in this system (81 km s^{-1} and 71 km s^{-1} for the primary and secondary, respectively; Hill, Fisher, & Holmgren 1990) suggests that manifestations of rotationally induced activity should be much more pronounced in this system compared to others. Gunn & Doyle (1997) and Newmark (1990) support this hypothesis, with the detection of excess emission in Hα, Ca II IRT, and Mg I *b* lines consistent with global emission from the system. Both conclude from their analyses that the emission arises from plagelike structures. We would expect that at such high rotation rates flaring will be a continuously occurring event. Indeed, Gunn & Doyle (1997) suggest that ER Vul could sustain continuous high levels of activity.

3.2. *Search for Phase-dependent Variations*

Because several of our observations were obtained over multiple stellar orbital periods, we searched for phase-dependent variations in the nonflaring sections of the light

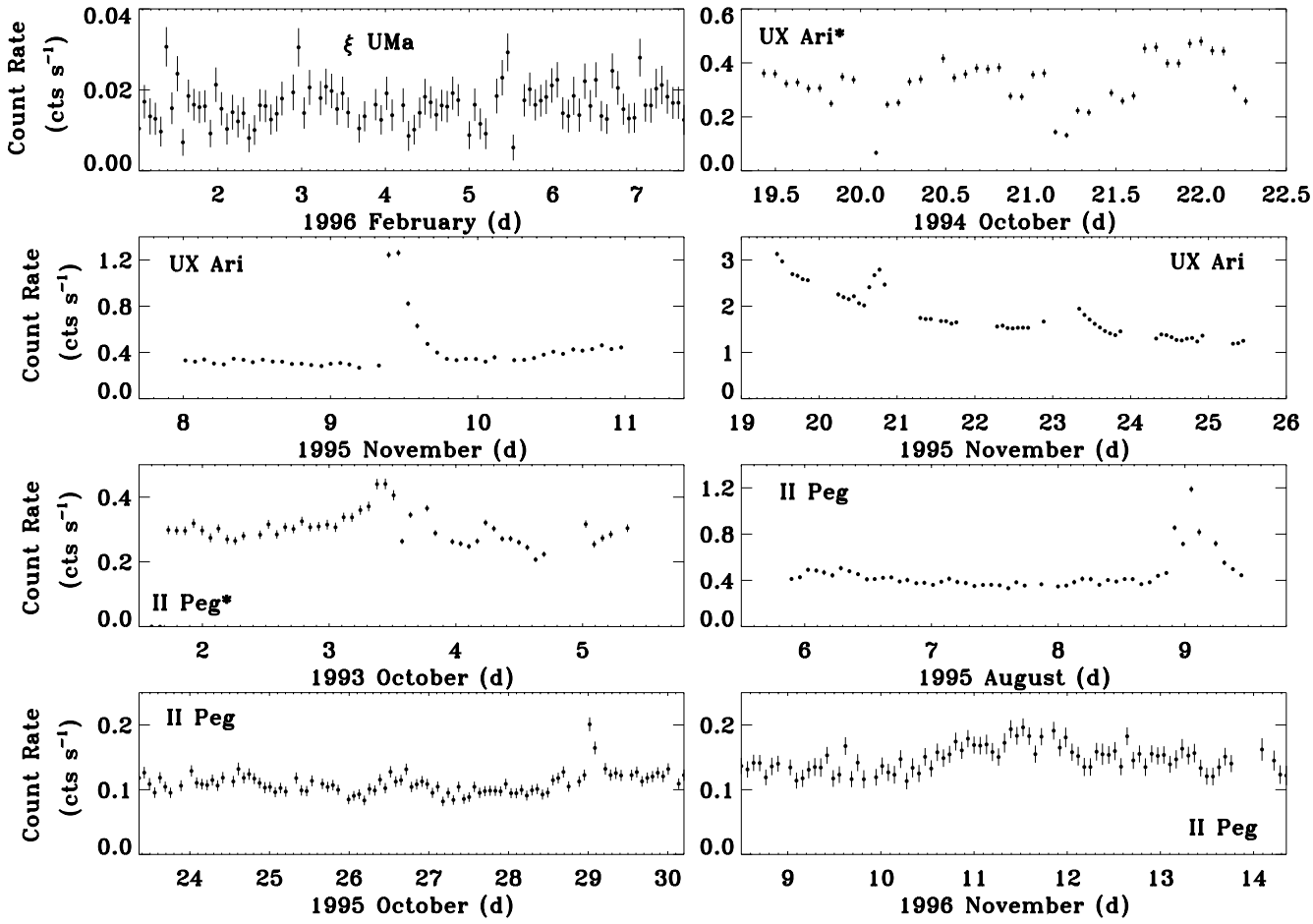


FIG. 3.—Same as for Fig. 1

curve. We proceeded as follows: for systems whose total N_{orb} exceeded 2, we removed any identifiable flares from the light curve. We then folded the light curve over the system's orbital period to obtain a phased light curve. The systems we examined were ER Vul (1993 September [DS/S]), CF Tuc (1994 August [DS/S]), V711 Tau (1992 October, 1993 September, 1994 August, and 1996 September combined [DS/S]), and II Peg (1995 October and 1996 November combined [RAP]). Since all these systems are synchronously rotating, the light curves are also phased with the stellar rotation. Our use of the term "phase-dependent variations" does not imply a particular geometry to explain the variability.

The CF Tuc 1994 August light curve shows clear evidence for modulation of the signal on the orbital period of 2.8 days (Figs. 6 and 7*b*). Gunn et al. (1997) originally analyzed this *EUVE* data set. Gunn et al.'s light curve (see their Figs. 5 and 6) contains a much larger binning—10, 000 s compared to 3000 s in our analysis. Our analysis excludes time bins that are substantially less than 3000 s and that hence would have larger error bars. Still, both reduction methods (Figs. 5 and 6 of Gunn et al., compared to our Fig. 7*b*) produce the same general light curve features: an enhancement of emission at low orbital phase ($\phi_{orb} \approx 0.2$–0.3) with a general decline at larger phases. Gunn et al. also point out a modulation of the EUV light curve at the orbital period and suggest that it, along with simultaneous radio modulation, indicates a region of intrabinary activity. When phased to P_{orb}, the points from different orbital cycles appear to be coherent for large portions of the light curve (Fig. 7*b*). There is some evidence for small flares occurring at smaller orbital phases.

Figure 7*a* shows the phased light curve of ER Vul for the 1993 September DS/S observation. The light curve does not show any evidence of being modulated over the multiple orbital periods of this observation. We interpret the variation as due to small-scale flaring, as discussed in § 3.1.

We examined a combination of the DS/S observations of V711 Tau, after removing flares in the 1993 September, 1994 August, and 1996 September light curves. Figure 7*c* shows the resulting phased light curve. There does not appear to be any structure in the light curve that is coherent over the $\sim$4 yr that the observations were made. Drake et al. (1994) investigated all-sky survey scanning observations and the 1992 October DS/S observations of V711 Tau, which were only $\approx$2 months apart. They find modulation of $\sim$40% in both light curves, which they interpret as either flarelike activity or rotational occultation of a bright coronal structure on the more active star. We do not find any evidence of modulation of the quiescent signal over the timescales of our observations. The minimum separation in time between observations is $\approx$11 months. Vogt et al. (1999) note the presence of a large, cool polar spot that persisted throughout the 11 years of their study, as well as numerous low-latitude spots that endured for less than 1 yr. If one interprets the quiescent emission as stemming from

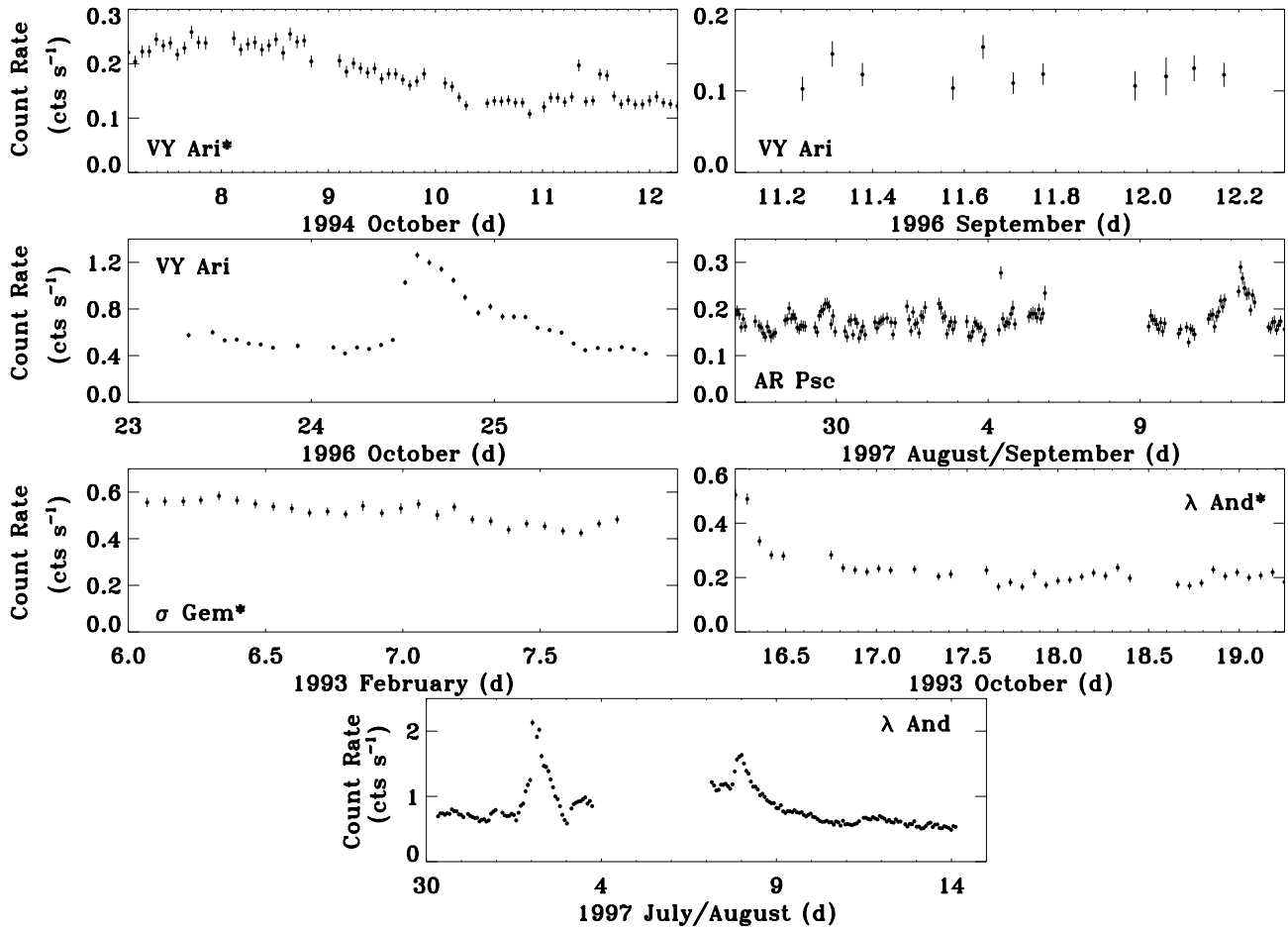


FIG. 4.—Same as for Fig. 1

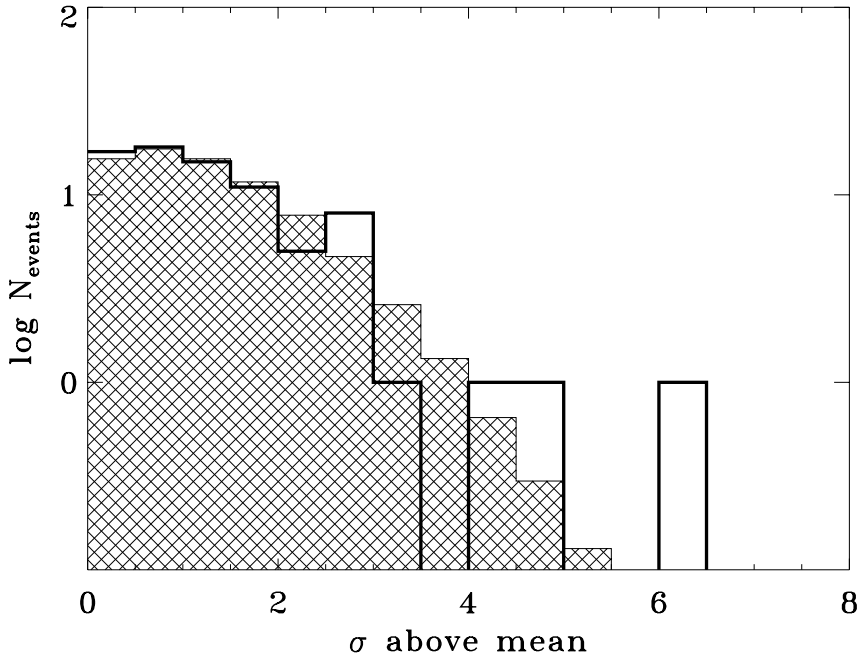


FIG. 5.—Histogram of variability in 1993 September and 1995 July ER Vul observations (*thick line*) compared to a Poisson distribution (*cross-hatched region*). The distribution of data fit the Poisson distribution reasonably well for variability $<2\,\sigma$. The large departures from the Poisson distribution at $>2\,\sigma$ suggest that another process is responsible for producing this observed distribution, most likely small-scale, stochastic flaring occurring almost continually on the system.

TABLE 2

FLARE PROPERTIES

System	Flare Start (YY/MM/DD)	$\phi_{orb,start}$	E_{flare} (10^{32} ergs)	τ_{rise} (hr)	τ_{dec} [a] (hr)	Δt_{flare} (hr)	$L_{flare,peak}$ (10^{28} ergs s^{-1})
σ^2 CrB	1994/02/17	0.514	13.	1.0 ± 0.03	2.2 ± 0.1	6.0	16.0
	1994/02/18	0.743	7.3	7.1 ± 1.6	8.4 ± 1.9	6.2	4.9
	1994/02/20.1	0.587	9.1	2.3 ± 0.2	6.3 ± 0.7	6.1	7.1
	1994/02/20.3	0.762	18.5	2.5 ± 0.2	3.3 ± 0.3, 18.9 ± 1.8	11.6	8.8
V824 Ara	1996/04/31.1	0.315	3.5	3.4 ± 0.8	3.6 ± 0.9	4.1	3.8
	1996/04/31.2	0.394	7.9	4.0 ± 1.1	15.9 ± 3.2	8.6	3.5
V815 Her	1996/06/16	0.278	7.7	5.6 ± 1.5	14.2 ± 3.2	10.4	3.3
	1996/06/26	0.655	22.	2.7 ± 0.5	3.4 ± 0.4, 35.2 ± 7.1	21.1	9.0
V711 Tau.....	1993/09/17	0.070	150.	8.2 ± 1.0	10.8 ± 0.6, 81.5 ± 11.3	40.2	21.8
	1993/09/18	0.701	110.	7.9 ± 0.4	8.3 ± 0.3, 32.3 ± 2.3	26.6	22.2
	1994/08/24	0.210	30.	3.0 ± 0.4	14.8 ± 1.3	13.5	9.4
	1994/08/25	0.744	18.	8.9 ± 1.2	17.2 ± 2.8	9.4	7.9
	1994/08/26	0.069	95.	9.2 ± 1.0	17.6 ± 1.0	30.1	13.5
	1996/09/04	0.769	14.	6.6 ± 1.3	16.6 ± 2.4	7.5	7.4
	1996/09/05	0.051	22.	5.6 ± 0.5	14.3 ± 1.2	10.8	9.0
	1996/09/07	0.859[b]	410.	23.9 ± 0.4	24.7 ± 0.4	83.6	20.2
	1996/10/12	0.050	310.	3.7 ± 0.2	7.7 ± 0.6, 21.6 ± 0.6	51.9	38.2
	1996/10/14	0.858	84.	22.6 ± 2.3	21.7 ± 2.7	34.3	11.0
UX Ari	1995/11/09	0.309	59.	1.1 ± 0.04	5.2 ± 0.2	10.7	30.6
	1995/11/20	0.056	290.	11.3 ± 1.0	23.0 ± 1.5	17.3	62.8
	1995/11/22	0.415	320.	15.5 ± 2.1	31.5 ± 1.5	25.1	50.2
II Peg	1995/08/8.8	0.352	13.0	2.0 ± 0.2	7.3 ± 1.5	4.8	14.2
	1995/08/8.9	0.372	49.0	2.8 ± 0.2	9.2 ± 0.3	13.1	19.8
	1995/10/28	0.413	22.0	3.2 ± 0.6	12.6 ± 2.1	9.6	10.2
VY Ari.....	1996/10/24	0.887	290	2.2 ± 0.2	15.6 ± 1.2, 26.1 ± 2.4	25.4	51.4
AR Psc	1997/09/10	0.082	10.2	7.0 ± 1.7	11.6 ± 2.7	8.6	4.2
	1997/09/11	0.378	43.3	51.3 ± 5.8	42.1 ± 4.8	32.4	5.2
λ And	1997/08/01	0.849	89.1	12.8 ± 0.3	6.9 ± 0.8, 17.0 ± 0.7	36.6	12.7
	1997/08/03	0.925	28.0	58.2 ± 9.8	40.3 ± 10.3	16.5	6.3
	1997/08/07	0.147	140.	15.9 ± 1.2	28.0 ± 1.6, 91.8 ± 2.7	71.8	10.2

[a] Where two numbers are given, the second refers to the decay time after a knee in the light curve.

[b] This is actually two flares that could not be separated. Rise time is for first flare, decay time is for second flare, energy is the total energy in both flares.

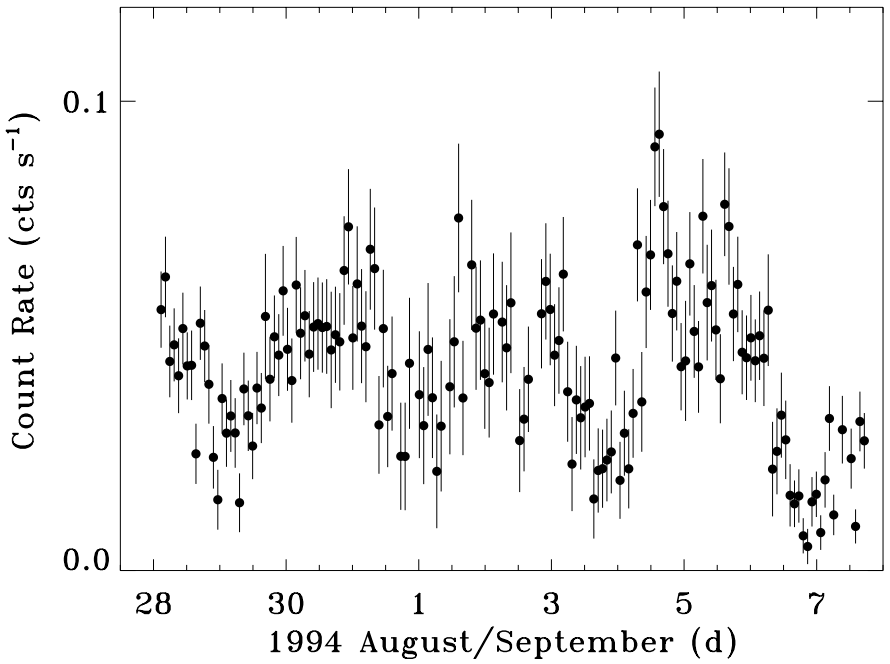


FIG. 6.—EUV light curve of CF Tuc. There is clear modulation of the signal at the 2.8 day orbital period.

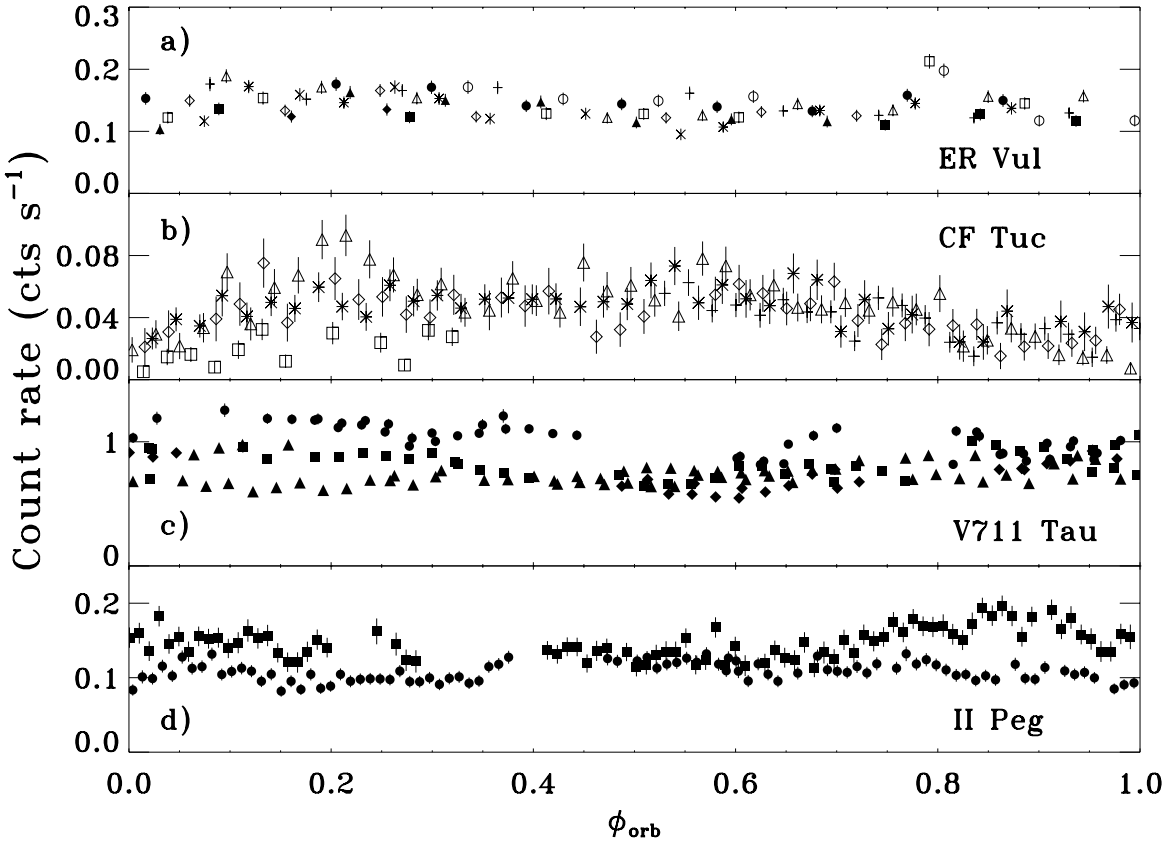


FIG. 7.—Phased EUV light curves of (*a*) ER Vul, (*b*) CF Tuc, (*c*) V711 Tau, and (*d*) II Peg. For (*a*) and (*b*), symbols indicate different orbital cycles over the course of the observation. In (*c*) and (*d*), symbols differentiate multiple observation epochs. Flares have been manually removed from the data. CF Tuc shows evidence for modulation of the emission on timescales of the orbital period; the other three systems do not show conclusive evidence for light curve coherence over multiple orbital periods or observation epochs.

active-region features, then we would not expect to see coherence of the emission on timescales longer than the lifetimes of individual active regions.

Two RAP observations of II Peg (1995 October, 1996 November) provided sufficient orbital coverage that we combined the two and investigated possible phase-dependent modulation, after removing a flare from the 1995 October light curve (Fig. 7*d*). There does not appear to be any structure in either light curve that suggests coherence over the $\approx$13 months between the two observations. Byrne et al. (1995) suggest from their study of the photosphere and chromosphere of II Peg that mean global chromospheric structures are stable on a 1.5 month timescale. Berdyugina, Ilyin, & Tuominen (1998) presented Doppler images for II Peg, near the epochs of our *EUVE* observations, that are dominated by high-latitude spots that migrate at approximately the same rate of $0\overset{\circ}{.}18$ day^{-1}.

3.3. *The Absence of Eclipses in Eclipsing Systems*

A few of the systems observed are partially or totally eclipsing systems. These are ER Vul, AR Lac, and CF Tuc. Christian et al. (1996) analyzed the Deep Survey light curve of AR Lac, the only totally eclipsing RS CVn system observed with *EUVE*, and claimed to see a decrease of $\sim$40% in intensity near primary eclipse. However, the light curve is contaminated by the dead spot on the Deep Survey detector; specifically, the times of eclipse occur while the observation was pointed in the dead spot. Because the pointing moved across the sharply varying sensitivity in the $\sim$20 pixel radius of the dead spot, we cannot be certain that any of the observed emission variation is due to eclipses.

The light curves of ER Vul and CF Tuc also do not show evidence for eclipses. We interpret the small-scale variability in ER Vul (on timescales $< P_{orb}$) as due to small-scale flaring events. We do not see any evidence for variation of the light curve at times of possible eclipses—the stochastic nature of the variability occurs at all orbital phases (see § 3.2 above). Fig. 7*a* shows the 1993 September observation of ER Vul phased to the orbital period and no eclipses are evident at conjunction ($\phi = 0.0$, $\phi = 0.5$). This constrains the emitting region to be of a larger physical size than the intrabinary separation. If the EUV emission were occurring on the surface of one star, the diminution of the emission during eclipse would be noticeable—the angle of inclination is $66\overset{\circ}{.}7$ and the radii are equal (Hill et al. 1990), with latitudes $>10^\circ$ being eclipsed (White et al. 1987). An even smaller percentage would be eclipsed were the emission to have an extent of 1–2 stellar radii.

The other partially eclipsing system, CF Tuc, also does not appear to show eclipses in the EUV. Gunn et al. (1997) demonstrated modulation of the flux at the orbital period. While there is an approximately two-thirds reduction in the count rate from a maximum of $\approx$0.06 counts s^{-1} at around $\phi = 0.6$ to $\approx$0.02 counts s^{-1} at $\phi = 1.0$, this reduction is not simply explained by a geometrical eclipse. The system's orbital inclination is 71° (Collier, Hearnshaw, & Austin 1981) and the cooler star's radius is roughly twice that of the hotter star (Coates et al. 1983). Roughly 24% of the K4 IV

star's surface area is eclipsed by the G0 V star; one would expect a shallow eclipse even if the emitting region were very compact. The predicted eclipse duration from optical light curves is $\Delta\phi \approx 0.1$ (Collier et al. 1981), while the observed variation occurs over the entire orbital period, not just at times of conjunction. We demonstrated in the preceding section evidence for coherence of the light curve over multiple cycles. The small orbital phases ($\phi < 0.3$) show a large scatter, which appears to be related to flaring events. Flares are visible in the light curve; no attempt to analyze these flares was made because of the strong underlying modulation of the flux.

4. ANALYSIS AND STATISTICS OF LARGE-SCALE FLARES

4.1. *Flare Analysis*

We identified and analyzed flares from the light curves of nine systems. Flares were identified in the initial light curve (binned into one point per satellite orbit) as definite excursions from the mean. Only flares that showed both a rise and a decay were analyzed. There were several instances in which an obvious flare decay was observed in the light curve (e.g., UX Ari: 1995 November 19); however, we required that the entire flare be present in the light curve for it to be included in subsequent analyses. For detailed analysis, the light curve was binned into six points per satellite orbit to enable better constraint of the rise and decay times. No flaring activity was observed on timescales between 500 and 3000 s. All flares occurred over several satellite orbits; we thus have no evidence of small-timescale (<3000 s) "microflaring" on these systems. The quiescent count rate was estimated from the light curve, and the flare was selected by eye starting from where the count rate departed from the quiescent value and ending where it rejoined the quiescent count rate. The *e*-folding times for rise and decay ($\tau_{\rm rise}$ and $\tau_{\rm decay}$) were determined from a logarithmic least-squares fit to the slope. For all flares, both the rise and decay are fit well by exponentials, showing the structured nature of the reconnection process. 1 σ errors are quoted in Table 2. For eight flares, two power-law slopes fit the decay with a lower χ^2_ν than a single power law (e.g., Fig. 8). In these cases, two power-law slopes were computed and two corresponding decay times were calculated. We determined the orbital phase of the flare start, total integrated energy in the flare, total flare duration, and peak flare luminosity (see Table 2). Using a representative spectrum of an RS CVn binary (V711 Tau, 1994 August observation) from the spectroscopy accompanying the DS/S pointed observations, we determined the median photon energy using the effective area for a particular detector/filter combination. We assume implicitly that flare spectra and nonflare spectra return the same median photon wavelength; i.e., the same spectral lines are observed in both cases. Spectral analysis shows this to be a good approximation (Brown & Gagné 1996). The EUV spectra of RS CVn binary systems are remarkably similar, independent of spectral type. Were the temperature structure on RS CVn systems to be more Sun-like, the observed EUV spectrum would change markedly; however, derived temperatures on RS CVn's appear to be consistent with each other, in the range of $1–3 \times 10^7$ K (Dempsey et al. 1993b). Hipparcos distances (ESA 1997) were used to determine total flare energy.

Figure 9 shows $\tau_{\rm rise}$ plotted versus $\tau_{\rm decay}$. We find a slowly increasing trend of $\tau_{\rm rise}$ with $\tau_{\rm decay}$ for flares that show single decay phases (*solid circles*). The least-squares fit to these points is $\tau_{\rm decay} = 1.95 + 1.13\tau_{\rm rise}$ and is shown in Figure 9 as a solid line. We computed the best fit to the flares that showed second decay times (*open squares* in Fig. 9); the fit is $\tau_{\rm decay,2} = 6.22 + 4.63\tau_{\rm rise}$ (*dashed line* in Fig. 9). This second set of decay times increases much more steeply with rise time than the single/first decay times. The Kolmogorov-Smirnov statistic (K-S test) for these two populations is 0.77, with a probability of 9.7×10^{-4} that the two are drawn from the same distribution. The existence of a corre-

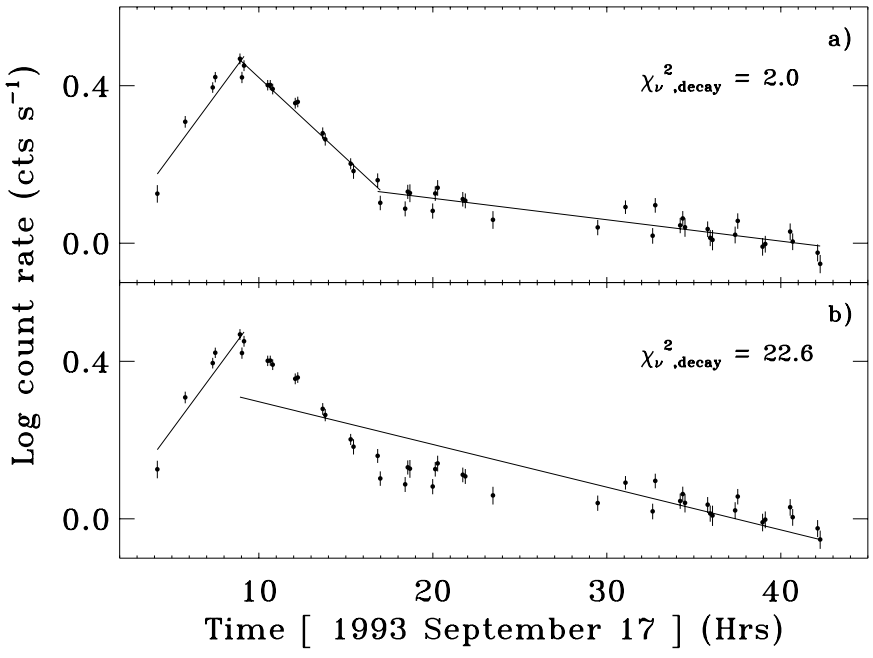


FIG. 8.—(*a*) Broken power-law fit and (*b*) single power-law fit to a flare occurring on V711 Tau. The χ^2_ν values show that a broken power law, or a "knee" in the light curve, is a better fit to the data than a single power law.

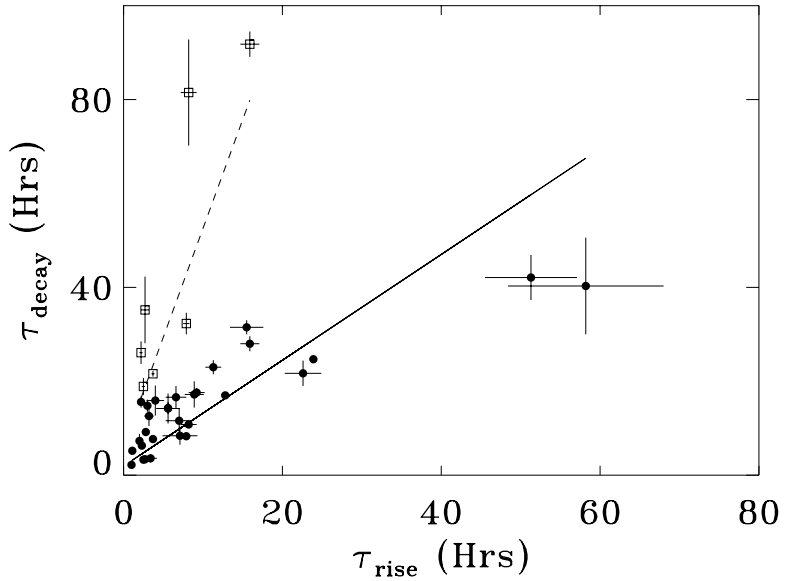


FIG. 9.—Flare rise times vs. decay times for 30 flares analyzed. Error bars are 1 σ uncertainties in the least-squares fit to the flare light curve. Filled circles represent flares that showed a single decay phase, or the first decay phase in instances in which two decay phases were present. Squares are the second e-folding time when two decay phases were present. Solid line is a fit to the first decay phase. Dashed line is a fit to the second decay phases. The K-S statistic reveals that these are two distinct populations; see text.

lation between the flare rise time and second decay timescale implies a physical connection between the two events. The physical cause of this change in decay rate is unclear: possibly the flare reconnection passes from one set of magnetic structures to another of substantially different scale, or a different energy dissipation (or deposition) mechanism becomes important, or the evolution of the flaring volume leads to a suppression of the radiative losses and lengthening of the decay rate. It is unlikely that the change is due to unrelated random flares because of the correlation observed.

We find a positive correlation between the flare energy and flare duration. Figure 10 plots the two quantities; the solid line is a least-squares fit, producing a power-law dependence of index 1.42 ($E_{\rm flare} \propto \Delta t^{1.42}$). This illustrates the prevalence of energetic, long-duration flares on these systems. We also compare the integrated flare luminosity against the quiescent luminosity for the flares studied. Figure 11 shows the correlation and resulting fit as a solid line. The integrated flare luminosity depends on the quiescent luminosity as $\log L_{\rm flare} = -1.33 + 1.05 \log L_{\rm quiescent}$, with a χ^2_ν of 0.44. The dashed line compares this fit to a one-to-one correlation. Previous studies of red dwarf flare stars showed a linear correlation between the mean flare power in the U-band and the stars' quiescent X-ray luminosity (Skumanich 1985; Doyle & Butler 1985). Pallavicini et al. (1990) find an increasing trend between total X-ray flare luminosity and quiescent X-ray luminosity for a sample of solar neighborhood flare stars observed with *EXOSAT*. These systems are either single stars or main-

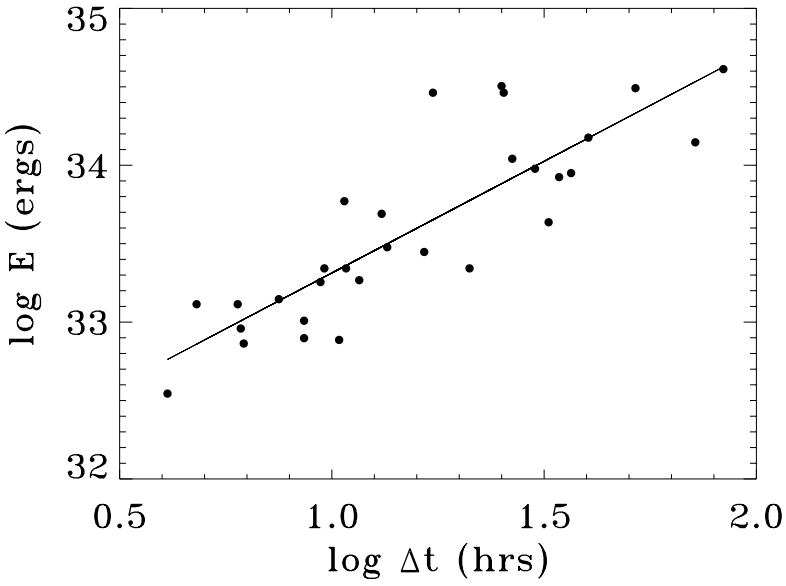


FIG. 10.—Flare energy plotted vs. flare duration. Solid line is a least-squares fit to the data, given by $\log E = 31.89 + 1.42 \log \Delta t$

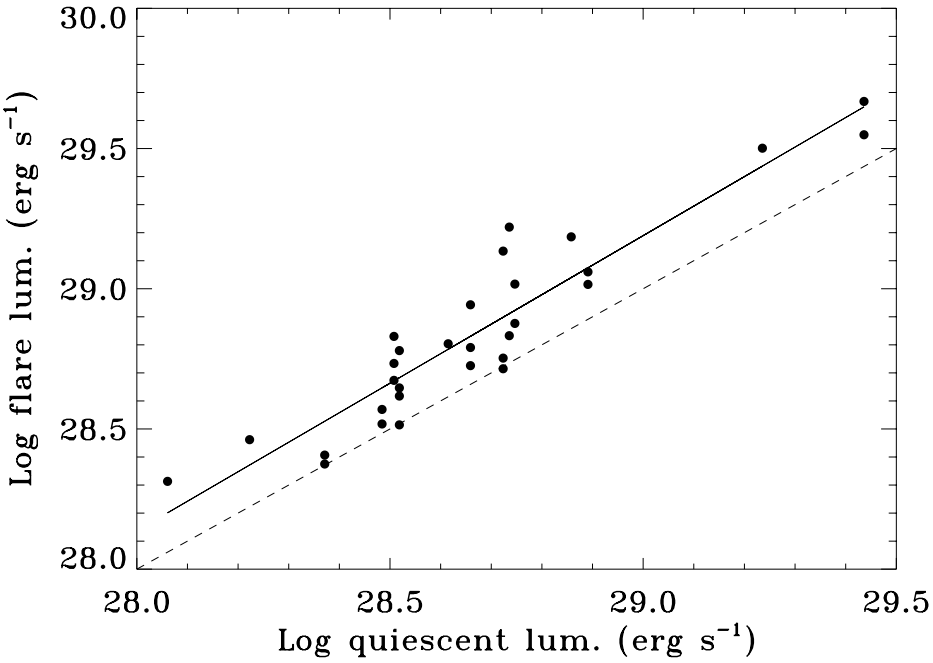


FIG. 11.—Integrated flare luminosity vs. quiescent luminosity. Solid line is fit to the data given by log (flare lum.) = −1.33 + 1.05 log (quiescent lum.). The χ^2_ν fit is 0.44. Dashed line is a line of equality between the two luminosities.

sequence binary stars of the BY Draconis type. We find a result similar to that of Pallavicini et al. (1990), although in our sample the quiescent luminosities cover the same magnitude range as the flare luminosities (the X-ray flare luminosities in Pallavicini et al. are 1 order of magnitude greater than the quiescent luminosities). Solar studies (Pearce et al. 1992) show a tight, positive correlation between the background X-ray (1–8 Å) flux and the number of solar Hα flares, with a power-law dependence of 1.1. Our result bolsters the conclusion that the energy of coronal flares is related to the ambient stellar activity level; more active systems (those systems that display larger amounts of quiescent luminosity) have more energetic flares on them. For RS CVn systems, in which chromospheric and coronal emission is saturated, the quiescent luminosity is probably the maximum that it can be. It is possible that the close agreement between flare and quiescent luminosity could be due to the saturated nature of these systems.

4.2. *Distribution of Flare Energies*

We plot a cumulative number distribution of flares as a function of flare energies (Fig. 12), assuming that all the systems obey the same intrinsic flare energy distribution. For flare energies between $\sim 10^{32.9}$ and $10^{34.5}$ ergs, the distribution follows a power-law fit, given by $N_>(E) = 19.84E^{-0.6}$ with a rollover in the distribution at around $10^{32.9}$ ergs. The dashed line in Figure 12 shows the extension of our fit at smaller energies, where our flare information suffers from incompleteness effects (note the rollover in the distribution for these energies). Hard X-ray studies of solar flares (Kucera et al. 1997) and soft X-ray studies of flare stars (Collura, Pasquini, & Schmitt 1988; Pallavicini et al. 1990) also reveal the same shape. Previous studies also fitted an underlying distribution of the form

$$N_>(E) = kE^{-\alpha}$$

and find power-law slopes α of 0.7 (Kucera et al. 1997), 0.7 (Pallavicini et al. 1990), and 0.5 (Collura et al. 1988). These numbers are consistent with our value of 0.6.

4.3. *Flaring as a Function of System Properties*

Flares on V711 Tau are numerous enough to permit a statistical treatment. We examined whether the distribution of flare onsets on V711 Tau is random with orbital phase. This system does dominate our collection of flares, having 10 of the 30 flares analyzed. Even with the large amount of satellite time required to assemble all flare data ($\approx$0.4 yr), we are still at the small-number limit when determining possible flare phase preferences for individual systems. We constructed a distribution for each bin of the phase distribution and compared it to a Poisson distribution with the same mean as the original distribution of flares. This procedure tests the hypothesis that the flares are randomly distributed, by collapsing the phase information and investigating the number distribution of flares. The distribution on V711 Tau is consistent with a Poisson distribution of the same mean; the K-S statistic is 0.33, with a 72% chance that the two are drawn from the same distribution. We therefore cannot conclude that the distribution of the 10 flares observed on V711 Tau occur at preferential phases. Research on optical flares on UV Cet stars seems to indicate nonrandomness in flaring rates (Lacy, Moffett, & Evans 1976; Pazzani & Rodonò 1981; Doyle et al. 1990).

Figure 13*a* plots the normalized peak flare luminosity against orbital period. We find a decreasing trend with orbital period. We compute the Spearman rank-order correlation coefficient and find a coefficient of −0.21, which is significant at the 74% level for this sample size. Previous attempts to characterize RS CVn coronal emission also determined that decreasing X-ray emission (normalized to the bolometric luminosity) was found for increasing orbital period (Walter & Bowyer 1981; Dempsey et al. 1993a). This relation was found for *quiescent* emission, however. Our

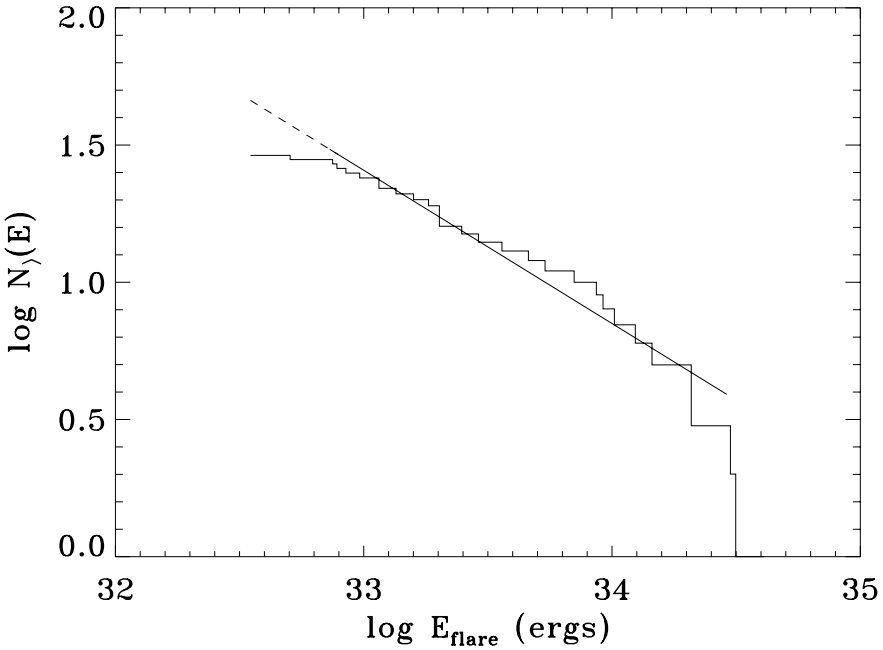


FIG. 12.—Flare distribution as a function of energy. Solid line is a least-squares fit to the distribution between $10^{32.9}$ and $10^{34.5}$ ergs. The slope of the power-law fit is -0.6. At energies $<10^{32.9}$ the data suffer from incompleteness effects.

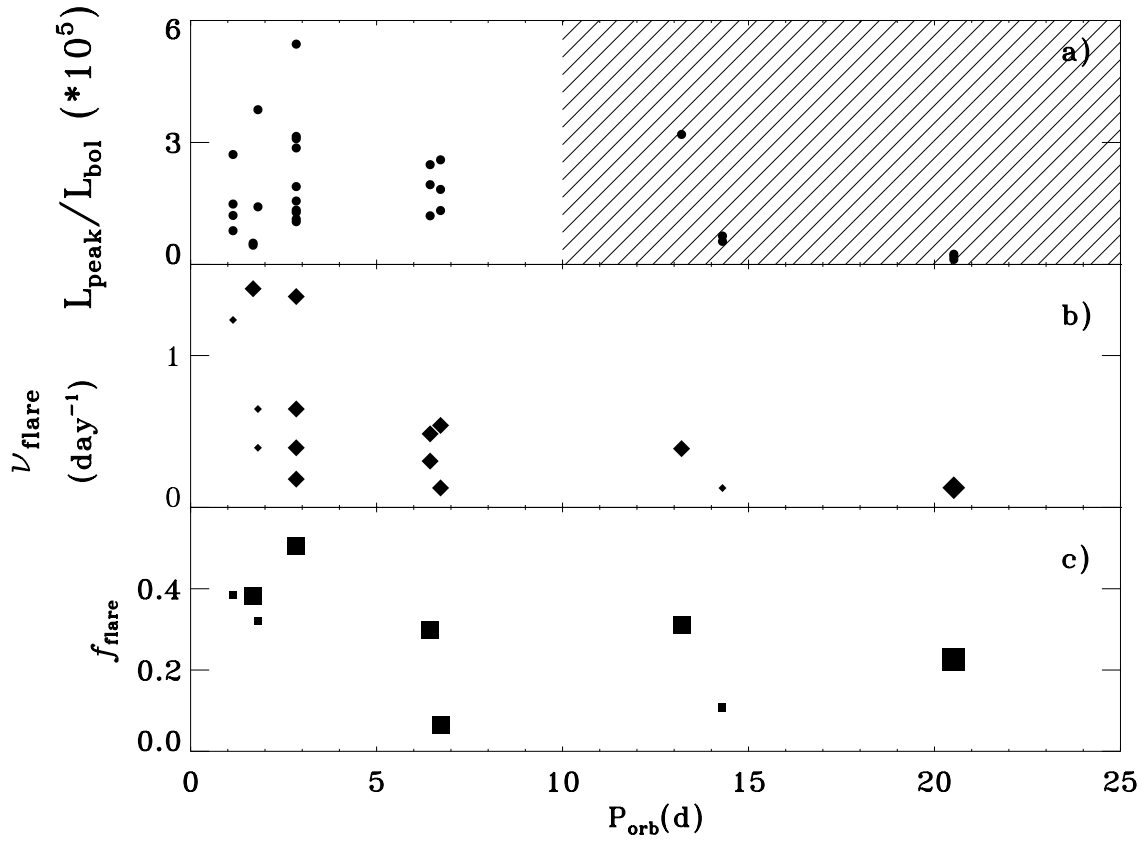


FIG. 13.—(*a*) Normalized peak flare luminosity as a function of orbital period. This trend is analogous to that found by Walter & Bowyer (1981) and Dempsey et al. (1993a) for quiescent emission from RS CVn systems. Hatching indicates the region where the systems are asynchronously rotating. (*b*) Observed flaring frequency as a function of orbital period. Flare frequency ν_{flare} is defined in § 4.2. There is a general trend of decreasing ν_{flare} with increasing P_{orb}. Size of diamond indicates evolutionary status. For systems with $P_{orb} > 10$ days, we do not have observations over enough of an orbital period to be confident of the flare frequency. We also suffer from lack of observations of these longer period RS CVn systems. (*c*) Fraction of observation time system was in a flaring state, as a function of orbital period. The average is ≈ 0.3.

sample size is admittedly smaller than those of the two surveys mentioned above; however, the greatly increased exposure times of our *EUVE* observations compensates in our ability to discern flaring and quiescent variations over a significant course of an orbital period (and in many cases, more than one orbital period). We do suffer from a lack of observations of longer period systems, but the trends we describe above reveal themselves even for short period systems, for which we do have a significant amount of data. Our result is analogous to the rotation-activity relation found in Walter & Bowyer and Demsey et al., whose results are for quiescent emission in RS CVn systems while ours are for flaring emission.

We also investigated frequency of flares as a function of orbital period. We define $\nu_{\rm flare}$ as

$$\nu_{\rm flare} = \frac{\text{number of flares}}{(t_{\rm exp}/\epsilon)},$$

where the number of flares is the number that were analyzed, i.e., that displayed both a rise and a decay time. Figure 13*b* plots the flare frequency versus $P_{\rm orb}$. There is a general trend of decreasing $\nu_{\rm flare}$ with increasing $P_{\rm orb}$; past $P_{\rm orb} = 10$ days, we suffer from small-number statistics and lack of complete (or near-complete) orbital coverage. The Spearman rank-order correlation coefficient is -0.78, with a significance at the 99.94% level. The range in frequency is from ~ 0.1 to 1.5 day^{-1}. The trend for systems with small orbital periods to have larger flaring frequencies stems from the increase in rotation rate for these tidally locked systems. The fast rotation drives more activity, creating regions of higher shear that could magnetically recombine and produce more flares than the more slowly rotating, longer orbital period systems.

Another parameter we examine is the fraction of time observed that was spent in a flaring state, $f_{\rm flare}$. We define $f_{\rm flare}$ according to

$$f_{\rm flare} = \frac{\sum \Delta t_{i,\rm flare}}{(t_{\rm exp}/\epsilon)}.$$

Figure 13*c* shows $f_{\rm flare}$ plotted against $P_{\rm orb}$. We find only a general trend, again exacerbated by a very small number of observations of the longer period ($P_{\rm orb} > 10$ days) systems and the shortness of these observations when compared to the orbital periods. $f_{\rm flare}$ shows as much variation on individual systems as across the span of orbital period; V711 Tau at $P_{\rm orb} = 2.84$ days spent $>90\%$ of the observed time during 1993 September flaring, while during the 1992 October observation, no large-scale flares were detected. The average fraction of time the stars were observed in a flaring state is ≈ 0.3. We report four flaring megaseconds, among 10 Ms of observations not contaminated by the dead spot. Flaring seems to be a preferred state for these systems.

4.4. *Evidence of Sympathetic Flaring*

We find that six sets of large-scale flares occur close enough in time to be considered "sympathetic." These pairs are σ^2 CrB: 1994 February 17 and 18; σ^2 CrB: 1994 February 20.1 and 20.3; V824 Ara: 1996 April 31.1 and 31.2; V711 Tau: 1996 September 4 and 5; V711 Tau: 1996 September 7; and II Peg: 1995 August 8.8 and 8.9. The two flares on V711 Tau on 1996 September 7 occurred so close together in time that we cannot adequately separate the start time for the second flare from the end time for the first flare. For three of the six pairs, the second flare appears to be of longer duration than the first, with roughly twice the energy of the first flare (in the case of II Peg 1995 August, the second flare is almost 4 times more energetic). We believe these phenomena are related to the much debated "sympathetic flares" on the Sun (Pearce & Harrison 1990). In this scenario, a flare in one active region stimulates flare activity in a removed active region through a disturbance that propagates through the solar atmosphere. Moreton waves (Moreton 1960), which are waves propagating outward from a flare site after flare onset, might be possible carriers of the disturbance to further removed active regions. Studies of optical flares on UV Cet stars indicate evidence for periodicities and sympathetic flaring (Panagi & Andrews 1995; Doyle et al. 1990).

4.5. *Flare Morphology*

We find a number of unusual flare morphologies in these systems, which are not readily explained using the two-ribbon solar flare model. In this model, both the rise and decay are part of the "gradual" phase of the flare (longer wavelength radio observations respond to the impulsive flare phase; Jones et al. 1996; Brown et al. 1996). The rising phase corresponds to filling of the coronal loop; the decay phase is associated with either cooling of the loop or sufficient loop expansion that the density and hence the emissivity drops. We find (see § 4.1, Fig. 9) that flare rise times can be comparable to or larger than the flare decay times. This is not a feature of two-ribbon solar flares. These flares are of long duration (>4 hr), with several flares displaying extremely long durations (greater than $0.5P_{\rm orb}$ and as great as $1.2P_{\rm orb}$). The emitting region must be physically extended, in order that the flare can be observed without diminution over a significant fraction of the orbital period. Previous research seems to suggest the same result (Jones et al. 1996; Gunn et al. 1997).

Eight of the flares analyzed were fit better by two power-law decays than by a single one (Fig. 8). These second decay phases are statistically different from the single decay phases (see § 4.1, Fig. 9). The timescales corresponding to the second decay phase are much longer than either typical single decay phases or the accompanying first decay phase. The "knee" in the light curve separates a faster initial flare decay from a much longer lived flare decay. While the exact physical cause of this change in decay rate is unclear, it is an important diagnostic of the physical changes occurring in the flaring region, as the correlation between rise time and second decay timescale suggests. There is no apparent trend with orbital period of systems that show two decay phases in flare light curves; both the shortest (σ^2 CrB, $P_{\rm orb} = 1.14$ days) and longest period (λ And, $P_{\rm orb} = 20.52$ days) systems that showed large-scale flares demonstrated two decay phases in at least one of their flares.

There were a few flares that demonstrated a sustained level of approximately constant emission at the peak of the EUV flare (Fig. 14). These flare "plateaus" can last for several hours (Fig. 14 shows sustained emission for ~ 5 hr before decaying). While only a small number of these plateaus were observed (four of 30), they all occurred on V711 Tau. This system was observed for the longest of all the systems in our study. Similar behavior was observed on AD Leo, which Hawley et al. (1995) interpreted using a quasi-static loop model. The appearance of plateaus is a good diagnostic of the reconnection process, as reconnection

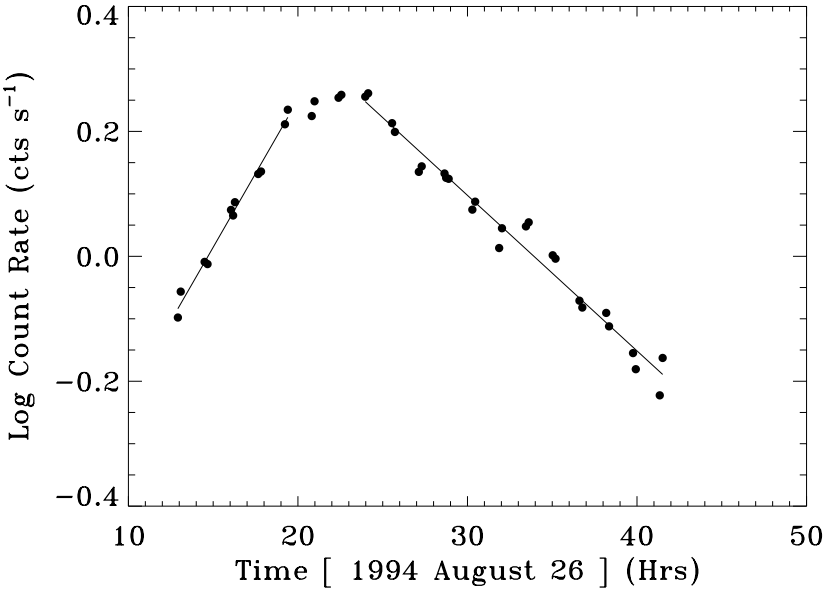


FIG. 14.—Example of a plateau in the flare light curve of V711 Tau. The flare sustained a maximum value for ≈5 hr before decaying. Total flare duration is 30.1 hr.

must balance the loop expansion to sustain a constant luminosity. We imagine that such a scenario would be uncommon and note that this occurs for only a small number of the flares analyzed.

5. SUMMARY

We have examined EUV emission from RS CVn binaries. All of the systems show evidence for variability, despite a lack of large-scale flares in many light curves. One system, CF Tuc, shows emission variation on the order of the orbital period. ER Vul, the shortest period system in our study ($P_{orb} < 1$ day), displays small-scale stochastic variability. We interpret this as evidence of small flares; the emission is neither phase modulated nor due to eclipses in the system. Light curves of two partially eclipsing systems (CF Tuc and ER Vul), do not display evidence of eclipses. Because of an unexplained periodicity in *EUVE* DS/S data of close to 1 day, we advise caution in interpreting periodicities in *EUVE* photometry that are of this order.

Our analysis of 30 large-scale flares reveals that flares on RS CVn systems are long-duration flares. Given the disparity between the solar analogue of two-ribbon flares and the flares seen on these systems, we think it highly unlikely that these flares are simply scaled-up versions of two-ribbon solar flares. Many flares show long rise times compared to the decay timescale. There is a small but significant sample of flares that show two decay phases, the second of which must be related to some physical change in the flaring process. The integrated flare energy correlates well with the flare duration, with a dependence of $\Delta t^{1.42}$. The integrated flare luminosity shows an almost 1:1 correspondence with the quiescent luminosity. The one system for which flares are numerous enough to permit an examination of the flare onset phase distribution, V711 Tau, is consistent with flare onsets being randomly distributed in time. We find a decreasing trend of normalized flare luminosities with orbital period, in analogy with previous results for quiescent emission from RS CVn systems. Flare frequencies range from 0.1 to 1.5 day^{-1}, with a slight decreasing dependence on orbital period. The RS CVn systems observed were in a flaring state for 40% of the total *EUVE* satellite observation time that was uncorrupted by dead spot observations. Flaring is a common phenomenon on these systems and is probably inevitable given the significant amounts of new emerging magnetic flux and the observed optical spot migration within an existing packed magnetic configuration. We examine the cumulative flare distribution as a function of energy and fit the distribution with a power-law slope of index −0.6 and cutoff $10^{32.9}$ ergs. Sympathetic flaring is a common occurrence in our observations; we also note the existence of unusual flare morphologies.

This work is supported by NASA grants NAG5-2259, NAG5-4735, and NAG5-3226. We would like to thank R. Dempsey for the opportunity to examine the V824 Ara data while it was still proprietary. R. A. O. would like to thank the staff scientists at the Center for *EUVE* Astrophysics for their helpful discussions on data reduction. Many thanks are owed to Graham Harper, Phil Bennett, Tom Ayres, and Jeffrey Linsky for their helpfulness in interpreting the data. We also thank Marc Gagné for allowing us to use his light curve and spectral *EUVE* software for the data reduction. We thank the referee, Alastair Gunn, for helpful comments on the manuscript.

REFERENCES

Berdyugina, S., Ilyin, I., & Tuominen, I. 1998, in ASP Conf. Ser. 154, Cool Stars, Stellar Systems, and the Sun, ed. J. Bookbinder & R. Donahue (San Fransisco: ASP), 1952
Bopp, B. W., Saar, S. H., Ambruster, C., Feldman, P, Dempsey, R., Allen, M., & Barden, S. C. 1989, ApJ, 339, 1059
Bowyer, S., Lieu, R., Lampton, M., Lewis, J., Wu, X., Drake, J. J., & Malina, R. F. 1994, ApJS, 93, 569
Brown, A., & Gagnè, M. 1996, in UV and X-ray Spectroscopy of Astrophysical and Laboratory Plasmas, ed. K. Yamashita & T. Watanabe (Tokyo: Universal Acad.), 101
Brown, A., Skinner, S. L., Stewart, R. T., & Jones, K. L. 1996, in Magnetodynamic Phenomena in the Solar Atmosphere: Prototypes of Stellar Magnetic Activity, ed. Y. Uchida, et al. (Dordrecht: Kluwer), 279
Byrne, P. B. 1989, Sol. Phys., 121, 61

Byrne, P. B., et al. 1995, A&A, 299, 115
Catalano, S., & Frasco, A. 1994, A&A, 287, 575
Christian, D. J., Drake, J. J., Patterer, R. J., Vedder, P. W., & Bowyer, S. 1996, AJ, 112, 751
Coates, D. W., Halprin, L., Sartori, P. A., & Thompson, K. 1983, MNRAS, 202, 427
Collier, A. C., Hearnshaw, J. B., & Austin, R. R. D. 1981, MNRAS, 197, 769
Collura, A., Pasquini, L., & Schmitt, J. H. M. M. 1988, A&A, 205, 197
Dempsey, R. C., Linsky, J. L., Fleming, T. A., & Schmitt, J. H. M. M. 1993a, ApJS, 86, 599
Dempsey, R. C., Linsky, J. L., Schmitt, J. H. M. M., & Fleming, T. A. 1993b, ApJ, 413, 333
Doyle, J. G., & Butler, C. J. 1985, Nature, 313 378
Doyle, J. G., van den Oord, G. H. J., Butler, C. J., & Kiang, T. 1990, A&A, 232, 83
Drake, J. J., Brown, A., Patterer, R. J., Vedder, P. W., Bowyer, S., & Guinan, E. F. 1994, ApJ, 421, L43
Endl, M., Strassmeier, K. G., & Kürster, M. 1997, A&A, 328, 565
ESA. 1997, The Hipparcos and Tycho Catalogues, ESA SP-1200 (Noordwijk: ESA)
Gagné, M., Valenti, J. A., Linsky, J. L., Tagliaferri, G., Covino, S., & Güdel, M. 1999, ApJ, submitted
Giampapa, M. S., Golub, L., & Worden, S. P. 1983, ApJ, 268, L121
Güdel, M., Linsky, J. L., Nagase, F., & Brown, A. 1999, ApJ, 511, 404
Gunn, A. G., & Doyle, J. G. 1997, A&A, 318, 60
Gunn, A. G., Migenes, V., Doyle, J. G., Spencer, R. E., & Mathioudakis, M. 1997, MNRAS, 287, 199
Haisch, B., Strong, K. T., & Rodonò, M. 1991, ARA&A, 29, 275
Hall, D. S. 1976, in IAU Colloq. 29, Multiply Periodic Phenomena in Variable Stars, ed. W. S. Fitch (Dordrecht: Reidel), 287
Halpern, J. P., & Marshall, H. L. 1996, ApJ, 464, 760
Hatzes, A. P., Vogt, S. S., Ramseyer, T. F., & Misch, A. 1996, ApJ, 469, 808
Hawley, S. L., et al. 1995, ApJ, 453, 464
Hill, G., Fisher, W. A., & Holmgren, D. 1990, A&A, 238, 145
Jones, K. L., Brown, A., Stewart, R. T., & Slee, O. B. 1996, MNRAS, 283, 1331
Kucera, T. A., Dennis, B. R., Schwartz, R. A., & Shaw, D. 1997, ApJ, 475, 338
Kürster, M., & Schmitt, J. H. M. M. 1996, A&A, 311, 211
Lacy, C. H., Moffett, T. J., & Evans, D. S. 1976, ApJS, 30, 85
Linsky, J. L. 1991, Mem. Sci. Astron. Italiana, 62, 307
Malina, R. G., & Bowyer, S. 1991, in Extreme Ultraviolet Astronomy, ed. R. F. Malina & Bowyer (New York: Pergamon Press), 397
Malina, R. F., et al. 1994, AJ, 107, 751
Mewe, R., Kaastra, J. S., van den Oord, G. H. J., Vink, J., & Tawara, Y. 1997, A&A, 320, 147
Miller-Bagwell, A., & Abbott, M. 1995, *EUVE* Guest Observer Center Data Products Guide
Mitrou, C. K., Mathioudakis, M., Doyle, J. G., & Antonopoulou, E. 1997, A&A, 317, 776
Moreton, G. E. 1960, AJ, 65, 494
Newmark, J. S. 1990, Ph.D. thesis, Pennsylvania State Univ.
Ortolani, A., Maggio, A., Pallavicini, R., Sciortino, S., Drake, J. J., & Drake, S. A. 1997, A&A, 325, 664
Ottmann, R., & Schmitt, J. H. M. M. 1994, A&A, 283, 871
Pallavicini, R., Serio, S., & Vaiana, G. S. 1977, ApJ, 216, 108
Pallavicini, R., Tagliaferri, G., & Stella, L. 1990, A&A, 228, 403
Panagi, P. M., & Andrews, A. D. 1995, MNRAS, 277, 423
Pazzani, V., & Rodonò, M. 1981, ApSS, 77, 347
Pearce, G., & Harrison, R. A. 1990, A&A, 228, 513
Pearce, G., Harrison, R. A., Bromage, B. J. I., & Pickering, A. G. M. 1992, A&A, 253, 601
Schrijver, C. J., Mewe, R., van den Oord, G. H. J., & Kaastra, J. S. 1995, A&A, 302, 438
Schmitt, J. H. M. M., Stern, R. A., Drake, J. J., & Kürster, M. 1996, ApJ, 464, 898
Singh, K. P., White, N. E., & Drake, S. A. 1996, ApJ, 456, 766
Skumanich, A. 1985, Australian J. Phys., 38, 971
Strassmeier, K. G., Hall, D. S., Fekel, F. C., & Scheck, M. 1993, A&AS, 100, 173 (CABS)
Vilhu, O., & Walter, F. M. 1987, ApJ, 321, 958
Vogt, S. S., Hatzes, A. P., Misch, A. A., & Kürster, M. 1999, ApJS, in press
Walter, F. M., & Bowyer, S. 1981, ApJ, 245, 671
White, N. E., Culhane, J. L., Parmar, A. N., & Sweeney, M. A. 1987, MNRAS, 227, 545
White, N. E., Sanford, P. W., & Weiler, E. J. 1978, Nature, 274, 569
Zhai, D. S., Foing, B. H., Cutispoto, G., Zhang, R. X., Catala, C., Char, S., Zhang, X. B., & Jankov, S. 1994, A&A, 282, 168
Zirin, H., MacKinnon, A., & McKenna-Lawlor, S. M. P. 1991, Solar Interior and Atmosphere, ed. A. N. Cox, et al. (Tucson: Univ. Arizona Press), 964